Flight Safety of Transport Aircraft during Landing with Crosswind Effects

(民航機降落時受側風影響之飛航安全)

Ray C. Chang (臧瑞傳) [1] and Szuying Tan (譚嗣瀛) [2]
Professor[1] and Assistant Professor[2]
Bing-Rong Tsai (蔡秉融) [3] and Xiang Wang (王翔) [3]
Reserch Assistant [3]
Department of Aviation Mechanical Engineering (航空機械系)
China University of Science and Technology (中華科技大學)
Project No: MOST 104-2221-E-157-003-

ABSTRACT

Aircraft landing in crosswind effects has been a safety problem for all types of aircraft. The runway veer-off event due to crosswind has been of great concern for the aviation community. The main objective of this research is to present fuzzy-logic modeling (FLM) technique to establish flight control models with the function of nonlinear dynamic inversion based on the datasets from the flight data recorder (FDR) for the purpose to provide improved control strategy. Specific examples involving a twin-jet transport with rolling motion before touchdown and runway veer-off event due to crosswind effects after touchdown are illustrated. It is shown that flight control models can execute flight simulations of improved control strategy. The simulated results can provide the mitigation concepts and avoid flight accident of runway veer-off for the transport aircraft with crosswind effects.

Keywords：Runway veer-off; crosswind effects; fuzzy-logic modeling (FLM); Flight Data Recorder (FDR) nonlinear dynamic inversion

摘 要

飛機降落時遭受到的側風的影響，一直是所有類型飛機 共同的安全議題 。因此側風的影響偏離跑道之意外事件，目前是航空界極為關注之問題。本論文旨在展示如何使用飛行 紀錄 器(FDR)之飛航資料及 模糊邏輯建模(FLM)技術來建立具備非線悫性動態反算功能之飛行控制模型；以飛行控制模型來提供 操控的改善策略。一架雙噴射發動機在著陸前有滾轉運動及著陸後因受側風的影響而導致偏離跑道意外事故為本文具體之範例。它展示，模糊邏輯飛行控制模型可以進行改善控制策略的模擬，模擬結果可以提供緩解觀念和避免民航飛機因側風的影響而導致的偏離跑道之意外事故。

關鍵字：偏離跑道、側風效應 、模糊邏輯建模 、飛行紀錄器(FDR)、非線悫性動態反算

I. INTRODUCTION

The aerodynamic database in flight simulators and design of autopilots of aircraft are mainly based on flight test data in nominal flights. These data consist of those required for aircraft certification. Traditional methods for flight data analysis, such as the maximum likelihood method (MMLE) [1 & 2] and the least-square or the stepwise regression method [3], are all based on assumed functional relations in aerodynamics, and when coupled with flight dynamic equations, correct and accurate dynamic response to strong varying crosswind is not guaranteed. A popular method of data analysis is that of Extended Kalman Filter (EKF) [4 & 5]. The filter is to smooth the data based on kinematic equations [6], in some cases with constraint on static nonlinear data. The corresponding dynamic characteristics are linearized with respect to the static data. Therefore, with the EKF the question of how to keep the unknown unsteady aerodynamic effect remains

Unsteady aerodynamic effects on flight dynamic variables mainly arise from the lag in flow field which fails to follow the motion. The so-called flow field includes the aircraft vortex wakes. For example, wakes of a descending aircraft will not assume their position and strength as assumed in static conditions before the aircraft would move down further. Therefore, the instantaneous control power may be affected. Near the ground, since the wake cannot penetrate the ground plane, it has a tendency to stay above the ground to induce a complex aerodynamic environment. Other off-nominal flights may be induced by adverse weathers, preceding aircraft’s vortex wakes, ice accretions, pilot’s actions, etc.

A strong varying crosswind is the type of wind field with varying magnitude and/or direction as encountered by an aircraft. The dynamic response to it frequently involves roll oscillation. If it is of the type of a gust, the aircraft will roll and the ensuing motion depends on how a pilot will respond. The present paper will develop a control law to suppress such oscillation with fuzzy-logic nonlinear dynamic inversion for a twin-engine transport aircraft.

The same transport aircraft ran off the runway after touchdown because of crosswind encountered [7]. The fuzzy-logic modeling (FLM) technique was employed to establish unsteady aerodynamic models by using the flight data from flight data recorder (FDR). The fuzzy-logic aerodynamic models were demonstrated to exhibit directional instability, unstable yaw damping, and loss of control effectiveness due to varying crosswind in the final several seconds in flare [7]. Although the fuzzy-logic aerodynamic models have robustness and nonlinear interpolation capability in predicting the degradation in stability and control characteristics, it cannot provide the necessary control strategy to avoid runway veer-off event (i.e. running off through the side of runway). To avoid runway veer-off event due to crosswind, again the FLM technique to establish flight control models based on the data from flight data recorder (FDR) will be employed. The present paper will demonstrate the necessary and appropriate application of rudder and aileron controls.

II. NUMERICAL METHOD DEVELOPMENT

Since the flight control models are established by using flight data, modeling technique is important and need to be carefully considered. The present method is related to control law development, so that the FDR data (i.e. the flight data) are directly employed to be more realistic.

A. Fuzzy-Logic Technique

Modeling procedures start from setting up numerical relations between the input (i.e. flight variables) and output (i.e. flight operations or aircraft response). To obtain continuous variations of predicted results, the present method is based on the internal functions, instead of fuzzy sets [8-10], to generate the output of the model.

System identification in the present paper includes two tasks: one is the model structure identification, and the other one is to identify the parameters that represent their corresponding model structures. The present modeling method was first developed by Takagi & Sugeno in 1985 [11], and later in 1995, Tan & Xie [12 & 13] applied the theory to simulate microelectronic processes with very good accuracy. The present paper is based on the modeling technique suggested by Tan & Xie [14]. This technique was first applied to aviation technology in 1997 and later to flight data [15-17]. An application of this modeling technique to examine aeroelastic effects of a transport aircraft was presented in reference [18]. A detailed description of the fuzzy-logic algorithm is available in reference [19] and is summarized in this section of the present paper.

The FLM method takes advantage of correlating multiple parameters without assuming explicit functional relations among them. The algorithm employs many internal functions to represent the contributions of fuzzy cells (to be defined later) to the over-all prediction. The internal functions are assumed to be linear functions of input flight parameters as follows [19]:

$$P^i = y_i(x_1, x_2, \cdots, x_r, \cdots x_k) = p_0^i + p_1^i x_1 + \cdots + p_r^i x_r + \cdots p_k^i x_k \tag{2.1}$$

where p_r^i, r =0, 1, 2,…, k, are the coefficients of internal functions y_i, and k is number of input variables. In Eq. 2.1, y_i is the estimated defected angle of flight control operation or value of dynamic response, and x_r are the variables of the input data. The numbers of the internal functions (i.e. cell’s numbers) are quantified by the membership functions.

With the internal function chosen in a linear form, the fuzzy-logic model resembles the multiple linear regression method. What makes the fuzzy-logic model unique is that it is in a form of fuzzy cell structure composed of linear equations. In other words, there are different numbers of cells corresponding with each input variable. The values of each input variable in the modeling, such as the angle of attack, are divided into several ranges, each of which representing a membership function with $A(x_r)$ as its membership grade, like a weighting factor. A fuzzy cell is formed by taking one membership function from each variable. The total number of cells is the number of possible combinations by taking one membership function from each input variable. For every cell, it has a fuzzy rule to guide the input and output relations. The rule of the i-th cell [19] is stated as:

if x_1 *is* $A_1^i(x_1)$*, and* x_2 *is* $A_2^i(x_2)$*, and ... , and* x_k *is* $A_k^i(x_k)$*, then the cell output can be stated as Eq. (*2.1*).*

where $i = 1,2,...,n$ the index of the cells, n is the total number of cells of the model; $P^i(x_1, x_2, \cdots, x_r, \cdots x_k)$ is the internal function with parameters $p_0^i, p_1^i, ..., p_r^i, ... p_k^i$ to be determined, and $A_k^i(x_k)$ denotes the membership function for x_k. Each function covers a certain range of input variables.

For a given system with input variables $x_1, x_2, \cdots, x_r, \cdots x_k$ of one data point, the recorded values of each input variables are normalized by using

$$x_{r,norm} = \frac{x_r - x_{r,\min}}{x_{r,\max} - x_{r,\min}}, \quad r = 1,2,\cdots,k \tag{2.2}$$

Hereafter $x_{r,norm}$ is denoted by x_r for simplicity in description. The membership grading ranges are transformed into the domain [0, 1]; "0" meaning no effect from the corresponding internal function, and "1" meaning full effect. Generally, overlapped triangles are frequently the shapes used to represent the grades. A fuzzy cell is formed by taking one membership function from each variable. The output of the fuzzy-logic model is the weighted average of all cell outputs.

In each fuzzy cell, the contribution to the outcome (i.e. the cell output) is based on the internal function, Eq. (2.1). The final prediction of the outcome is the weighted average of all cell outputs after the process of reasoning algorithm. The output is estimated by the center of gravity method. For the j^{th} input ($x_{1,j}, x_{2,j}, ..., x_{r,j}, ..., x_{k,j}$), the output is as follows:

$$\hat{y} = \frac{\sum_{i=1}^{n} op[A^i(x_{1,j}), \cdots, A^i(x_{r,j}), \cdots, A^i(x_{k,j})]P^i}{\sum_{i=1}^{n} op[A^i(x_{1,j}), \cdots, A^i(x_{r,j}), \cdots, A^i(x_{k,j})]} \quad j = 1, 2, \ldots, m \tag{2. 3}$$

In Eq. (2.3), $op\left[A_1^i(x_{1,j}), ..., A_k^i(x_{k,j})\right]$ is the weighted factor of the i^{th} cell; and the index j of the data set, where j=1, 2, …, m, and m is the total number of the data records. The symbol "op" stands for product operator of its elements in the present paper.

There are two main tasks involved in the fuzzy-logic modeling process. One is the determination of p-parameters of the linear internal functions. The other is to identify the best structure of fuzzy cells of the model, i.e. to determine the best number of membership functions for each input variable in the modeling. The p-parameter~~s~~ is calculated with the gradient-descent method by minimizing the sum of squared errors (SSE) [19]:

$$SSE = \sum_{j=1}^{m} (\hat{y}_j - y_j)^2 \tag{2.4}$$

On the other hand, the structure of fuzzy cells is optimized by maximizing the multiple correlation coefficients:

$$R^2 = 1 - \frac{\{\sum_{j=1}^{m} (\hat{y}_j - y_j)^2\}}{\{\sum_{j=1}^{m} (\bar{y} - y_j)^2\}} \tag{2.5}$$

where $\hat{y}_j$ is the output of the fuzzy-logic model, y_j is the measured data, and $\bar{y}$ is the average value of all data.

The flight control model is defined by the values of p_r^i –coefficients. These coefficients are determined by minimizing SSE (Eq. 2.4) with respect to these coefficients. Minimization is achieved by the gradient-descent method with an iterative formula defined by:

$$p_{r,t+1}^i = p_{r,t}^i - \alpha_r \frac{\partial(SSE)}{\partial p_r^i} \tag{2.6}$$

where α_r is convergence factor or step size in the gradient method; subscript index t denotes the iterative sequence.

After simplification, Eq. (2.6) becomes

$$\frac{\partial(SSE)}{\partial p_r^i} = 2\sum_{j=1}^{m} (\hat{y}_j - y_j) \frac{\partial \hat{y}_j(x_{1,j}, ..., x_{k,j}, p_r^1, ..., p_k^n)}{\partial p_r^i} \tag{2.7}$$

Since the computed gradient tends to be small with Eq. 2.7 and involves matrix iteration so that the convergence is slow and time-intensive. To accelerate the convergence, the iterative formulas are modified by using the local squared errors to give:

For r=0,

$$p^i_{0,t+1} = p^i_{0,t} - 2\alpha_0(\hat{y}_j - y_j)\frac{op[A^i_1(x_{1,j}),\ldots,A^i_k(x_{k,j})]}{\sum_{s=1}^{n} op[A^s_1(x_{1,j}),\ldots,A^s_k(x_{k,j})]} \tag{2.7a}$$

and for r = 1, …, k,

$$p^i_{r,t+1} = p^i_{r,t} - 2\alpha_r(\hat{y}_j - y_j)\frac{op[A^i_1(x_{1,j}),\ldots,A^i_k(x_{k,j})]x_{r,j}}{\sum_{s=1}^{n} op[A^s_1(x_{1,j}),\ldots,A^s_k(x_{k,j})]} \tag{2.7b}$$

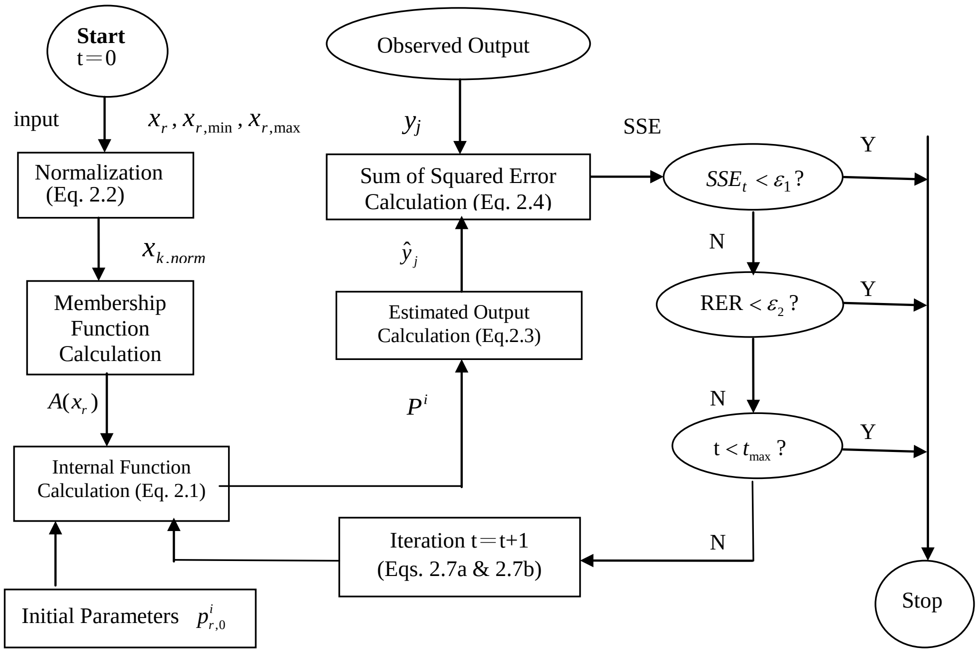

Fig. 2.1 Flowchart of parameter identification algorithm

In other words, Eqs. (2.7a) and (2.7b) are based on a point-iteration. The iteration during the search sequence stops when one of the following three criteria [19] is satisfied:

1) Cost=SSE_t = minimized

2) RER=$\frac{SSE_t - SSE_{t-1}}{SSE_t} < \varepsilon_2$

3) t=$t_{\max}$

In the above criteria, SSE_t is the sum of squared errors (SSE) being the cost function and RER= (cost_current - cost_previous)/cost_current to be denoted by "RER" (i.e. the relative error) for simplicity in descriptions; ε_2 is the required precision criteria. Fig. 2.1 is the flowchart of parameter identification algorithm.

Given membership functions and the training data, this parameter identification procedure can be applied to establish a fuzzy-logic model. Once the flight control models are set up, one can specify how the some input variables should vary to estimate the corresponding control law to achieve these specified behaviors.

B. Flight Control Model

A preprocessor is needed to re-arrange the flight variables in the dataset, and interpolate the variables if necessary by a monotone cubic spline [20]. For example, the FDR data can provide the necessary data to develop models for pilot training and flight control development. If flight test data are used, no further interpolation is necessary in most cases. To illustrate, the roll oscillation and runway veer-off problems will be considered. The following numerical models based on the FDR data in landing operation with dynamic ground effect may be generated:

$$\delta_a = f_2(\alpha, \theta, \phi, \dot{\phi}, \dot{\psi}, V_{cas}, \delta_f, a_y, V_{crw}, V_{tlw}, h_r, V_d) \tag{2.8}$$

$$\delta_r = f(\alpha, \theta, \phi, \dot{\phi}, \dot{\psi}, V_{cas}, \delta_f, a_y, V_{crw}, V_{tlw}, h_r, V_d) \tag{2.9}$$

where the parameter on left hand side of Eqs. (2.8) and (2.9) represents the aileron angle (δ_a) and rudder angle (δ_r). The flight variables on the right hand side represent angle of attack (α), pitch angle (θ), roll angle (ϕ), time rate of roll angle ($\dot{\phi}$), time rate of heading angle ($\dot{\psi}$), calibrated airspeed (V_{cas}), flap angle (δ_f), lateral acceleration (a_y), crosswind speed (V_{crw}), tailwind speed (V_{tlw}), radar altitude (h_r), and descent speed (V_d).

To develop flight control models, one or more dynamic variables (on the right-hand sides of the above expressions) are chosen as the enabling variables to achieve the desired dynamics. In the present case, the time rates of roll angle and yaw angle, in addition to the roll angles, are to be changed. Traditionally, the control laws are usually developed based on the roll and yaw rates on the rotating axes (i.e. “p” and “r”). Here, $\dot{\phi}$ is used because it will provide roll damping directly to the ϕ- motion. This is particularly important when ϕ, $\dot{\phi}$ and $\dot{\psi}$ have large amplitudes in roll oscillation. In the runway veer-off event, $\dot{\psi}$ is the enabling variable because it is the response directly related to rudder. However, associated with the specified change in $\dot{\psi}$, the lateral acceleration (a_y) should be changed as well. Therefore, the following sub-models are needed associated with Eq. (2.9):

$$a_y = f_1(\alpha, \theta, \phi, \dot{\psi}, V_{cas}, \delta_f, V_{crw}, V_{tlw}, h_r, V_d) \tag{2.10}$$

Another sub-model is that of $\dot{\phi}$:

$$\dot{\phi} = f_2(\alpha, \theta, \phi, \dot{\psi}, V_{cas}, \delta_f, a_y, V_{crw}, V_{tlw}, h_r, V_d) \tag{2.11}$$

When the aircraft is on the ground, $\dot{\phi}$ is small, but not zero, probably due to structural vibration. For the roll oscillation associated with Eq. (2.8), change in a_y is assumed negligible compared with the changes in enabling variables: ϕ, $\dot{\phi}$ and $\dot{\psi}$.

III. NUMERICAL RESULTS AND DISCUSSIONS

A. Flight Data

The main aircraft geometric and inertial characteristics are taken to be:

W = 533,790 N (120,000 lb)
S =112.32 m^2 (1209 ft^2), $\bar{c}$ = 3,41m (11.2 ft),
b= 32,89 m (107.9 ft)
I_{xx} = 2,507,963 $kg{\cdot}m^2$ (1,849,530 $slugs\text{-}ft^2$),
I_{yy} = 6,402,517 $kg{\cdot}m^2$ (4,721,620 $slugs\text{-}ft^2$)
I_{zz} = 8,569,733 $kg{\cdot}m^2$ (6,319,862 $slugs\text{-}ft^2$),
I_{xz} = 141,940 $kg{\cdot}m^2$ (104,676 $slugs\text{-}ft^2$)

The necessary data in the FDR to determine the flight characteristics for this transport is time (t), angle of attack (α), pitch angle (θ), roll angle (ϕ), heading angle (ψ), calibrated airspeed (V_{cas}), flap angle (δ_f), lateral acceleration (a_y), crosswind speed (V_{crw}), tailwind speed (V_{tlw}), radar altitude (h_r), and descent speed (V_d). Since the lateral acceleration (a_y) is a major flight variable of the present study about runway veer-off, while this parameter is recorded in 4-Hz resolution (i.e. 4 points per second), all other parameters are interpolated with a monotone cubic spline [20] to the same sampling rate. Although not considered here, the vertical acceleration is recorded in 8-Hz resolution. Therefore, eventually all variables are interpolated to 8-Hz sampling rate.

B. Analysis and Control of Roll Oscillation

Before the touchdown, the transport is subjected to both tailwind and crosswind with considerable magnitude in crosswind as shown in Fig. 3.1. It is well-known that varying crosswind would induce rolling motion. The rolling motion in crosswind effects and the corresponding aileron deflections of this transport will be studied through the predicted aileron angle (δ_a) of aileron control model. In the present study, the accuracy of the established aileron control model through FLM algorithm is estimated by the sum of squared errors (SSE) and the square of multiple correlation coefficients (R^2). The predicted aileron angles (δ_a) to compare with those of flight data in landing phase are presented in Figs. 3.2. The predicted values of aileron angle have a good agreement with the flight data.

In order to reconstruct the flight condition of this event, the datasets in landing phase from t=45233 to 45431 sec are used for the modeling. Before touchdown, the flight encountered gust-like crosswind (Fig. 3.1) with the resulting roll oscillation as shown in Fig. 3.3. Although the roll angles are small, the necessary aileron control may not too small because of the dynamic ground effect as indicated earlier.

The control laws are all based on the following structure:

$$\sum_{x+\dot{x}}[b+(x-b)f_c] \rightarrow \delta_x \tag{3.1}$$

where the summation means to combine the changes in the enabling variable (x), such as ϕ, and its associated time rate of change; b is the specified minimum value of "x" and f_c is the fraction to keep "x" above the minimum. The arrow sign implies dynamic inversion to determine the required control. The reason of doing this is to make the variation smooth so that the control is also smooth to avoid early control saturation. To reduce the roll angle (x = ϕ), the corresponding control law used is

b=2.0; f_c = 0.1

For x = $\dot{\phi}$ and $\dot{\psi}$, the same parameters are chosen. The prediction procedures are as follows, using roll control as an example:

1) Objective: to reduce the roll angle (ϕ) and improve the roll damping by selecting b = 2.0 and f_c = 0.1. In other words, the amount of ϕ above 2.0 deg is multiplied by 0.1. For $\dot{\phi}$, the amount above 2.0 deg/sec is also multiplied by 0.1. Since rolling is always accompanied by yawing, so that $\dot{\psi}$ is treated in the same way as $\dot{\phi}$.
2) If there are sub-models, then estimate the values of these sub-models due to the change in 1).
3) The aileron control needed to achieve the objective in 1) is calculated through the fuzzy-logic model representing Eq. (2.8).
4) Check whether the control exceeds the positive and negative limits. If true, revise the factors "b" and "f_c".

For the control of roll oscillation, the results are also shown in Fig. 3.3 (a). The maximum roll angle is slightly larger than 2.0 modified by f_c. The modified angular rates are compared with the original values in Fig. 3.4. Indeed, all angular rates are kept roughly within 2.0 deg/sec. The resulting aileron deflection indicates significant unsteady aerodynamic effect (Fig. 3.3(b)). That is, even though the first roll angle to be suppressed is larger than the second one, but the required aileron is smaller, because at the second one the aircraft is much closer to the ground. Note that the last point at t = 45405 sec. is the touchdown point. It turns out in this flight the aircraft descended faster than the normal flights, so that the dynamic ground effect near the ground should be more significant.

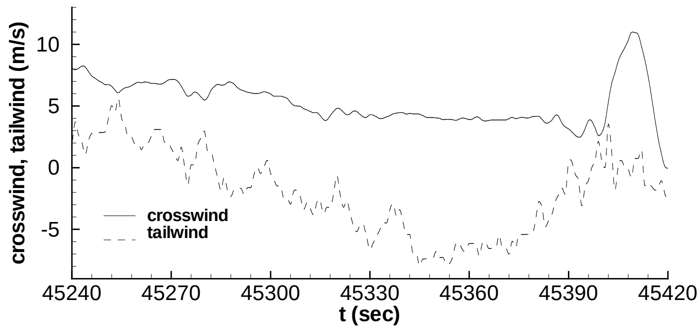

Fig. 3.1 Time history of wind field during landing

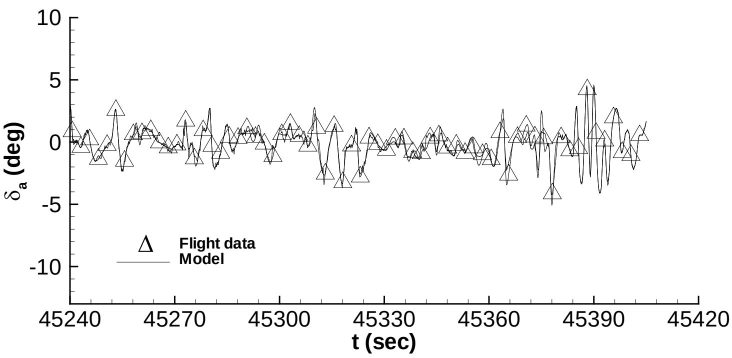

Fig. 3.2 Predicted aileron angle (δ_a) in landing phase based on FDR data

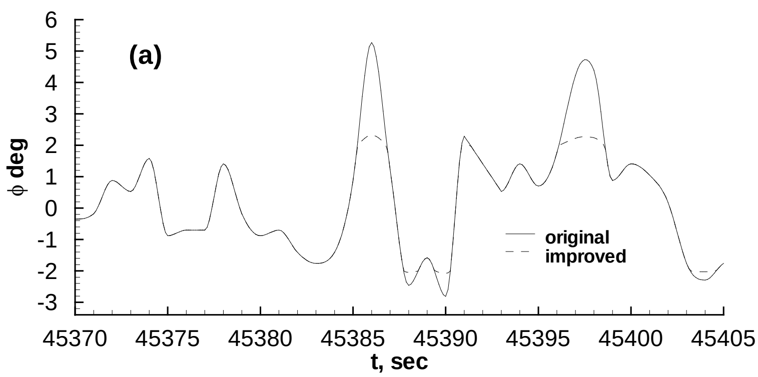

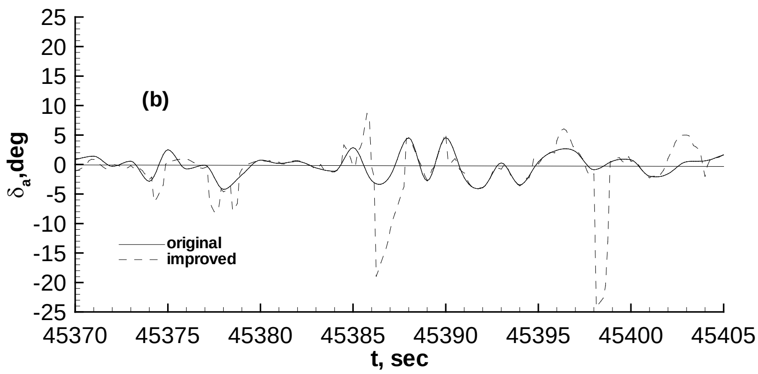

Figure 3.3 Roll oscillations of the subject aircraft in varying crosswind

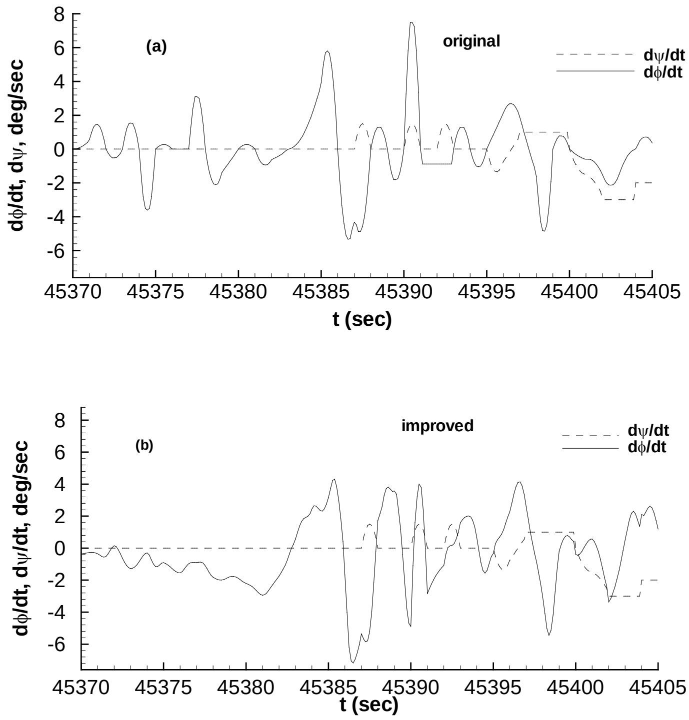

Figure 3.4 Modified angular rates compared with the original values

C. Analysis and Control of Runway Veer-off

About the potential runway veer-off, the main factor is the drift angle. If it is positive, the ground speed vector is to the right-hand side of the airspeed vector (represented by the heading angle). It appeared that the flight was normal without having veer-off possibility due to the variations of crosswind speed are from 8 to 3 m/s on the decrease, as shown in Fig. 3.1 and the heading angles with small variations, as presented in Fig. 3.5. The drift angle was about 3 degrees. However, after touchdown there was a strong 12 m/s (21kts) gust toward the right at around x=200 m, as shown in Fig. 3.6. Note. Negative tailwind is headwind and the distance of runway x=0 m is defined as the touchdown point. The positive gust reduces the heading angle, as it should be, but the heading angle immediately increases again, as presented in Fig. 3.5. Positive increase in heading angle plus the positive drift angle is the cause of runway veer-off. The critical point of motion trajectory on the runway is at x=520 m. Therefore, the aircraft should move back quickly toward the center line of the runway (i.e. y=0 m). On the contrary, the transport moves toward the outside of the runway boundary at x= 680 m, as shown in Fig. 3.7. The trajectory is estimated by integrating the ground speed to obtain the distance traveled

(Δs between two data points) and then determine the distance traveled along the heading direction (i.e. the x-component) and perpendicular to the heading direction (i.e. the y-component):

$$\Delta x = \Delta s * \cos(\Delta\psi + \delta_d) \tag{3.2}$$

$$\Delta y = \Delta s * \sin(\Delta\psi + \delta_d) \tag{3.3}$$

where $\Delta\psi$ is change in heading angle (an integrated value) from that at the touchdown point and δ_d is the drift angle available in the FDR data. Δs is estimated from integrating the ground speed:

$$\Delta s = \int_{t_{i-1}}^{t_i} V_g \, dt \tag{3.4}$$

where V_g is the ground speed and the integration is performed by a trapezoidal rule.

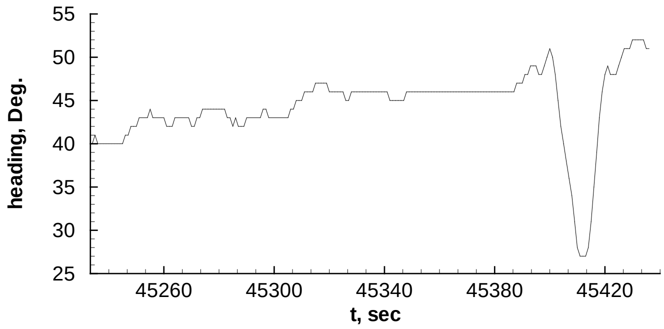

Fig. 3.5 Time history of heading angles during landing

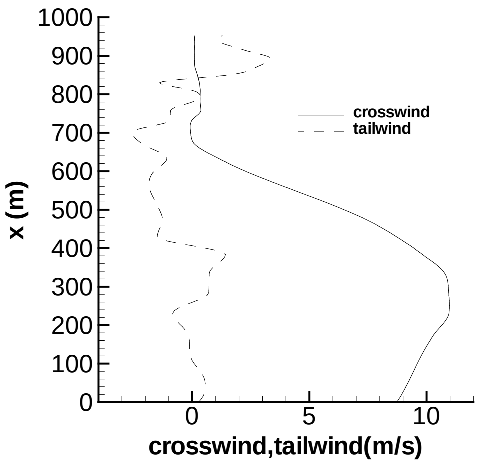

Fig. 3.6 Time history of wind field after touchdown

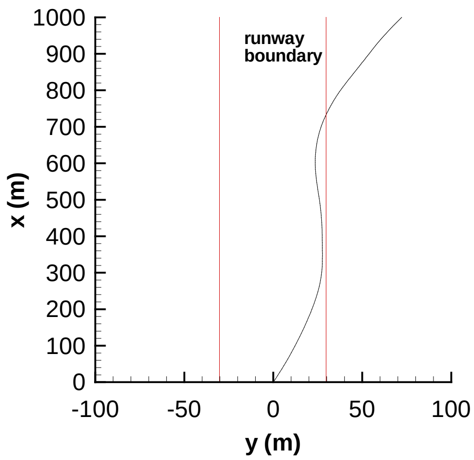

Fig. 3.7 Motion trajectory of runway veer-off event

D. Analysis of Model Predictions in Runway Veer-off

In the present study, the accuracy of the established yaw control models through FLM algorithm is estimated by the sum of squared errors (SSE) and the square of multiple correlation coefficients (R^2). The predicted rudder angle (δ_r), lateral acceleration (a_y), and time rate of roll angle ($\dot{\phi}$) to compare with those of flight data in landing phase are presented in Figs. 3.8, 3.9, and 3.10, respectively. The predicted values of rudder angle before and after touchdown have a good agreement with the flight data, especially in the time period after t= 45405 sec. The predicted values of lateral acceleration before and after touchdown have a good agreement with the flight data, except at the points of t= 45396 sec and t= 45410 sec. The predicted values of time rate of roll angle (Fig. 3.10) are slightly different from flight data in the time period after t= 45405 sec., still with an average of zero value as it should be theoretical because the aircraft was on the ground. One reason for this is that $\dot{\phi}$-data was not emphasized in modeling as soon as the aircraft was on the ground.

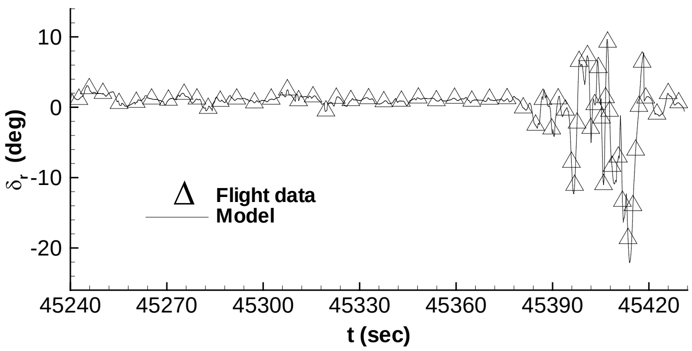

Fig. 3.8 Predicted rudder angle (δ_r) in landing phase based on FDR data

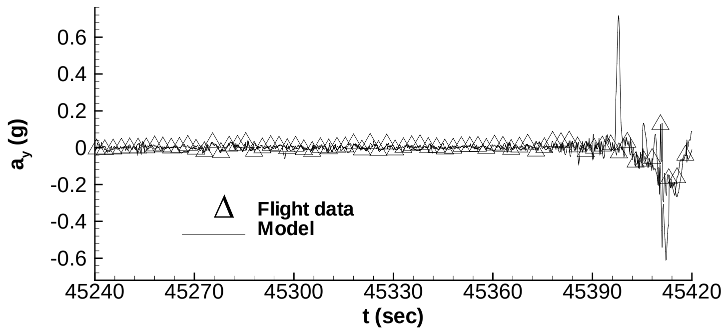

Fig. 3.9 Predicted lateral acceleration (a_y) in landing phase based on FDR data

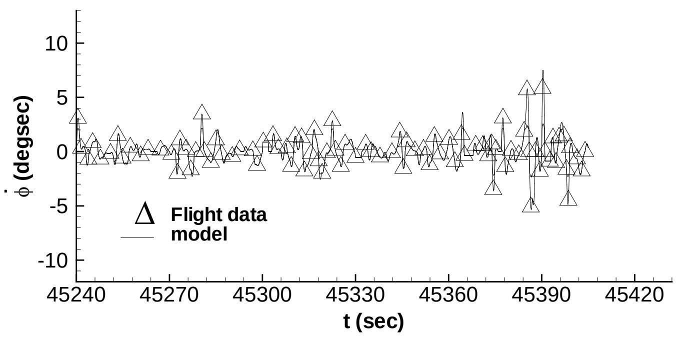

Fig. 3.10 Predicted time rate of roll angle ($\dot{\phi}$) in landing phase based on FDR data

E. **Root Causes of Runway Veer-off**

Initially, the aircraft was moving to the right because of positive drift angles (see later) after touchdown. So the rudder was deflected positively to generate negative time rate of heading angles, as presented in Fig. 3.11 and Fig. 3.12. The aircraft encountered a strong gust with the speed of 12 m/s toward the right after touchdown at around x=200 m, as shown in Fig. 3.6. The pilot quickly used the left rudder to move the aircraft to the left to correct the heading angles of aircraft. At around x=305 m in Fig. 3.6, a large positive crosswind occurred and this was countered by a negative rudder (right pedal) with some delay (by about 4 sec.), as shown in Fig. 3.11. This makes the time rate of heading angles more positive so that the aircraft moved to the right side continuously, as presented in Fig. 3.12. The rudder operations in heading angle corrections were not proper due to the wind direction suddenly changed from the tailwind to headwind at x=396 m. The critical point of runway veer-off was at x=520 m and toward the outside of the runway boundary at x= 680 m, as shown in Fig. 3.12.

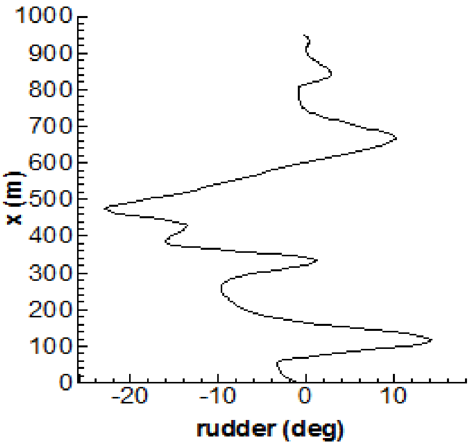

Fig. 3.11 Time history of rudder operations after touchdown

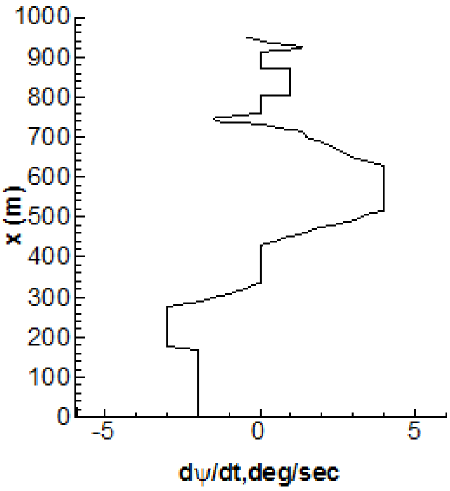

Fig. 3.12 Time history of time rate of heading angles after touchdown

Note that a positive crosswind would generate a positive side force and reduce the heading angle. Therefore, the increase in heading angle should be caused by the large negative rudder. A negative rudder would produce negative side force on the vertical tail and positive time rate of heading angle. Positive increase in time rate of heading angle plus the wind direction suddenly change from the tailwind to headwind should be the cause of runway veer-off event.

F. **Control Strategy in Runway Veer-off**

In a positive crosswind, the drift angle is positive and the airplane will move to the right side. To determine if veer-off can be avoided: A small -(dψ/dt) defined as $\Delta\dot{\psi}$ is imposed for positive crosswind or drift angle. The original and new time rates of heading angles are shown in Fig. 3.13. The solid line represents the specified (or improved) time rate of heading angles. To slow down the motion to the right side by making the time rate of heading angles slightly more negative (adding -0.20 deg/sec) until ($\Delta\psi+\delta_d$) becomes negative. At this point, $\Delta\psi$ is greater than δ_d in magnitude. Then $\Delta\dot{\psi}$ is made slightly more negative by adding -0.002 deg/sec to $\Delta\dot{\psi}$ at each data point to expand this negative region of ($\Delta\psi+\delta_d$). However, eventually $\Delta\psi$ will be more positive as shown in Fig. 3.14. To put a brake on the increasing positive $\Delta\psi$, it is simply assume that $\Delta\dot{\psi}$ = - 0.05 deg/sec when $\Delta\psi \geq 5.0$ deg. The resulting variation of drift angle, $\Delta\psi$ and rudder deflections is illustrated in Fig. 3.15. It is seen that the rudder variation is rapid and "erratic". The reason for the erratic rudder deflection is perhaps caused by the unsteady aerodynamic effect. That is, when the crosswind is strong enough, the aerodynamic performance of the vertical tail could be changed. The crosswind will blow the aircraft wake, including the engine exhaust, toward the vertical tail on the windward side. In addition, the airstream toward the vertical tail is always turbulent. Therefore the rudder control power would be significantly affected. A successful control strategy in unsteady flow field is to apply unsteady control deflections such as those displayed in the initial portion of Fig. 3.14 and Fig. 3.15.

The final improved trajectory is shown in Fig. 3.16. All these assumptions of numerical factors mentioned above are made to prove a point that if $\Delta\psi$, ($\Delta\psi+\delta_d$) and δ_d are made available to the pilot, it may be possible for the pilot to avoid the runway veer-off.

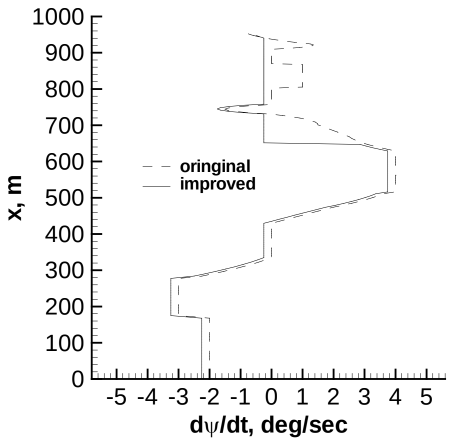

Fig. 3.13 Original and improved time rates of heading angles after touchdown

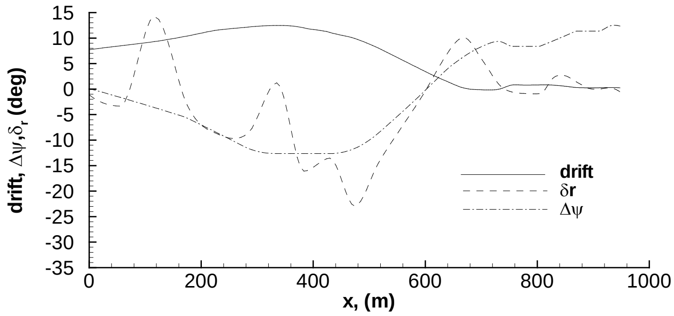

Fig. 3.14 Time history of original drift angle (drift), change in heading angle ($\Delta\psi$), and rudder angle (δ_r) after touchdown

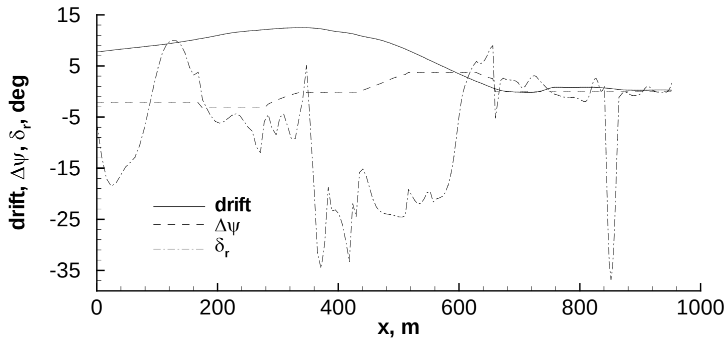

Fig. 3.15 Drift angle (drift), improved change in heading angle (Δψ) and rudder angle (δ_r) after touchdown

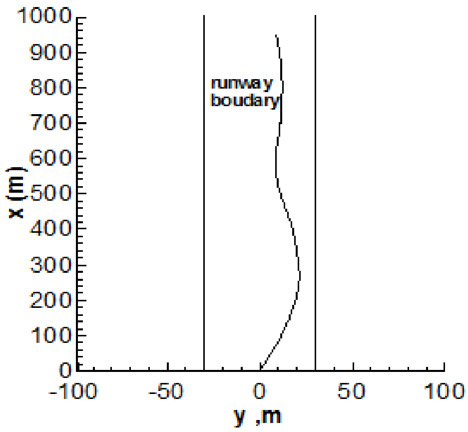

Fig. 3.16 Improved aircraft trajectory after touchdown at (x,y)=(0,0)

IV. CONCLUDING REMARKS

The main objective of this report was to present the development of flight control models based on the FLM method. The resulting models could keep implicitly the unsteady aerodynamic effect and hence realistically solve the mathematical problems in engineering. A twin-jet transport with roll oscillation before touchdown and runway veer-off event after touchdown due to crosswind was illustrated in this report. To improve the flight or prevent any accident, the necessary control law or strategy was developed based on a new method of Fuzzy-Logic Dynamic Inversion. The numerical results for control of roll oscillation indicated that indeed roll controls near the ground and away from the ground are significantly different in dynamic ground effect because of unsteady aerodynamics. In the problem of runway veer-off, it was also shown that to avoid the accident from happening, it was important to consider the unsteady aerodynamic effect as well. The latter might be generated from the interaction between a strong crosswind and the vertical tail to degrade the control capability. Since the currently employed simulator database was not capable of displaying such effects, pilot training would not be effective.

ACKNOWLEDGMENTS

This research project is sponsored by a grant, MOST 104-2221-E-157-003-, from Ministry of Science and Technology (MOST), Taiwan (ROC). The accomplishment in this project is part of the requirements set by the Aviation Safety Council (ASC), Taiwan (ROC).

REFERENCES

[1] Maine, R. E. and Iliff, K. W., User's Manual for MMLE3, a General FORTRAN Program for Maximum

Likelihood Parameter Estimation, NASA TP-1563, Nov. 1980.
[2] Maine, R. E., & Iliff, K. W., Application of Parameter Estimation to Aircraft Stability and Control, NASA Reference Publication No. 1168, NASA, USA, 1986.
[3] Klein, V., J., Batterson, G., and Murphy, P. C., Determination of Airplane Model Structure from Flight Data by Using Modified Stepwise Regression, NASA TP-1916, 1981.
[4] Gelb, A., *Applied Optimal Estimation*, M. I. T. Press, Cambridge, Massachusetts, USA, 1982.
[5] Minkler, G. & Minkler, J., *Theory and Application of Kalman Filter*, Magellan Book Company, Tucson, Arizona, USA, 1993.
[6] Chang, R. C., Ye, C. E., Lan, C. E., and Lee, Y. L., "Nonlinear and Dynamic Aerodynamic Models for Commercial Transport Aircraft with Adverse Weather Effects", *Mathematical Problems in Engineering*, Volume 2010, Article ID 924275, doi:10.1155/2010/924275.
[7] Weng, C. T, Ho, C. S., Lan, C. E, and Guan, M., "Aerodynamic Analysis of a Jet Transport in Windshear Encounter during Landing**,"** *AIAA Journal of Aircraft*, vol. 43, no. 2, 2006, pp. 419-427.
[8] Kuo, H. C., Hsu, Y. Y., "Distribution System Load Estimation and Service Restoration Using a Fuzzy Set Approach," *IEEE Trans. on PWRD*, Vol. 8, No. 4, 1993, pp.1950-1957.
[9] Ferrero, A., Sangiovanni S., and Zapitelli, E., "A Fuzzy Set Approach to Fault Type Identification in Digital Relaying," *IEEE Trans. Power Del.*, Vol. 10, No. 1, Jan. 1995, pp. 169–175.
[10] Montero, J., Gómez, D. and Bustince, H., "On the Relevance of Some Families of Fuzzy Sets," *Fuzzy Sets and Systems***,** Vol. 158, No. 22, 16, 2007, pp. 2429–2442.
[11] Takagi, T. and Sugeno, M, "Fuzzy Identifications of Systems and Its Applications to Modeling and Control," *IEEE Transactions on Systems, Man and Cybern*, Vol. SMC-15, No. 1, January/February 1985, pp. 116-132.
[12] Tan, J., Xie, H., and Lee, Y. C., "Efficient establishment of a fuzzy logic model for process modeling and control," *IEEE Transactions on Semiconductor Manufacturing*, Vol. 8, No. 1, February 1995, pp. 50-61.
[13] Xie, H., Mahajan, R. L., and Lee, Y. C., "Fuzzy logic models for thermally based microelectronic manufacturing process," *IEEE Transactions on Semiconductor Manufacturing*, Vol. 8, No. 3, August 1995, pp. 219-227.
[14] Joh, J., Chen, Y. H. and Langari, R., "On the stability issues of linear Takagi–Sugeno fuzzy models," *IEEE Transactions on Fuzzy systems*, Vol. **6**, Nov. 3, Aug. 1998, pp. 402–410.
[15] Wang, Z., Lan, C. E., and Brandon, J. M., "Fuzzy Logic Modeling of Nonlinear Unsteady Aerodynamics", AIAA Paper 98-4351, August 1998.
[16] Wang, Z., Li, J., Lan, C. E., and Brandon, J. M., "Estimation of Unsteady Aerodynamic Models from Flight Test Data", AIAA Paper 2001-4017, August 2001.
[17] Wang, Z., Lan, C. E., and Brandon, J. M., "Estimation of Lateral-Directional Unsteady Aerodynamic Models from Flight Test Data", AIAA Paper 2002-4626, August 2002.
[18] Chang, R. C. and Lan, C. E., "Structural Health Monitoring of Transport Aircraft with Fuzzy Logic Modeling," *Mathematical Problems in Engineering*, Volume 2013, Article ID640852, 2013, 11 pages.
[19] Lan, C. E. and Chang, R. C. , *Chapter 7 Fuzzy-Logic Analysis of the FDR Data of a Transport Aircraft in Atmospheric Turbulence*, Part 2, Fuzzy Logic–Emerging Technologies and Applications, InTech – 51000, ISBN 978-953-51-0337-0, March 16, 2012, Rijeka, Croatia.
[20] Huyuh, H.T., "Accurate Monotone Cubic Interpolation," *SIAM Journal on Numerical Analysis*, Vol. 30, issue 1, 1993, pp. 57-100.